Ladder physics in the spin fermion model

A. M. Tsvelik

Condensed Matter Physics and Materials Science Division, Brookhaven National Laboratory, Upton, New York 11973-5000, USA

A link is established between the spin fermion (SF) model of the cuprates and the approach based on the analogy between the physics of doped Mott insulators in two dimensions and the physics of fermionic ladders. This enables one to use nonperturbative results derived for fermionic ladders to move beyond the large-N approximation in the SF model. It is shown that the paramagnon exchange postulated in the SF model has exactly the right form to facilitate the emergence of the fully gapped d-Mott state in the region of the Brillouin zone at the hot spots of the Fermi surface. Hence, the SF model provides an adequate description of the pseudogap.

Introduction. The purpose of this Rapid Communication is (i) to establish a link between two successful phenomenological descriptions of the underdoped cuprates and (ii) to use it to obtain some different results. One description is based on the spin fermion (SF) model [1]; the other one is based on the analogy between the cuprate physics and the physics of fermionic ladders. Both approaches have been successful in describing different aspects of the cuprate physics. The SF model provides a natural platform for the description of the complicated phase diagram of the cuprates (see, for example, Ref. [2], and references therein). The merit of the ladder description, on the other hand, lies in its treatment of the pseudogap. In this approach, the formation of a pseudogap does not require any translational symmetry breaking, which is consistent with the experiments [3–5]. The ladder analogy was first put forward by Dagotto and Rice [6]; insights from the models of coupled ladders [7] eventually led to the popular expression for the single-electron Green's function [the so-called Yang-Rice-Zhang (YRZ) expression] [8].

The SF model describes electrons interacting with soft paramagnons in the vicinity of an antiferromagnetic quantum critical point (AF QCP). The strongest correlations are concentrated in the regions of the Fermi surface connected by the antiferromagnetic wave vectors $\mathbf{Q} = (\pm\pi, \pm\pi)$ (hot spots). The low-energy degrees of freedom are collective magnetic excitations and quasiparticles with a large Fermi surface. The model was conceived as phenomenological, but similar descriptions can be obtained from microscopic models, such as the model of weakly coupled Hubbard ladders [9] or the two-dimensional Hubbard model using dynamical mean field theory (DMFT) [10]. Below, I will demonstrate that the ladder physics is contained in the SF model. The effective dimensionality reduction related to the ladder physics is facilitated by the long-range exchange interaction mediated by the paramagnons.

The Hamiltonian of the SF model is

$$H = \sum_k \epsilon(k)\psi_\sigma^+(k)\psi_\sigma(k) + g\sum_{k,q} \psi^+(k+q)\boldsymbol{\sigma}\psi(k)\mathbf{S}(q)$$

$$+ \sum_q \frac{1}{2}\mathbf{S}(-q)\chi^{-1}(q)\mathbf{S}(q),$$

$$\chi^{-1}(q) = \chi_0^{-1}[\xi^2(\mathbf{Q}-\mathbf{q})^2 + 1]. \tag{1}$$

It has been shown that the frequency dependence of the spin susceptibility χ is generated by the quasiparticles and does not need to be included in the bare action [1].

In the standard approach, the spin fermion coupling is considered as a perturbation which generates significant effects only near the spots on the Fermi surface (FS) connected by the $\mathbf{Q}$ vector. The pieces of FS connected by the $\mathbf{Q}$ vectors are not nested. For the most recent applications of this approach, one can consult Ref. [2].

Ladder model approach. In this Rapid Communication, I will follow a different approach. I will assume that the spin fermion coupling is sufficiently strong and take as a starting point the FS which is nested at the hot spots. If the spectral gaps generated by the interaction are sufficiently large, then one can treat the deviation from the nesting as a perturbation. One can also speculate that the strong interactions will modify the shape of the Fermi surface to stabilize nesting to take advantage of the gap opening, as it happens in the commensurate antiferromagnetic state in Cr alloys [11] (see Fig. 1 and also Ref. [12]).

As I have stated above, due to the singular character of the spin-spin interaction, strong correlations occur only in the vicinity of the hot spots. The eight spots are divided into two quartets; in one quartet the spots from the opposite sides of the FS are connected by the wave vector (π, π) and in the other by the wave vector $(\pi, -\pi)$. To the first approximation, these two groups of hot spots can be considered independently.

It is convenient to use a tomographic projection and to introduce the operators

$$R_a(x) = \frac{1}{\sqrt{2\pi}}\int \psi(\mathbf{k}_R^a + k_\parallel \mathbf{e})e^{ik_\parallel x},$$

$$L_a(x) = \frac{1}{\sqrt{2\pi}}\int \psi(\mathbf{k}_L^a + k_\parallel \mathbf{e})e^{ik_\parallel x}, \tag{2}$$

where $\mathbf{k}_{R,L}^a \, a = \pm 1$ are coordinates of the hot sports in momentum space and $\mathbf{e} = (1,1)/\sqrt{2}$. Then, after integration over the spin variables, we obtain the following Hamiltonian density, describing the vicinity of the hot spots:

$$\mathcal{H} = iv_F \sum_{a=\pm 1, \sigma=\pm 1/2}(-R_{a\sigma}^+\partial_x R_{a\sigma} + L_{a\sigma}^+\partial_x L_{a\sigma}) + V,$$

$$V = -\gamma \sum_{a=\pm 1}(R_a^+\boldsymbol{\sigma}L_a + L_a^+\boldsymbol{\sigma}R_a)\sum_{b=\pm 1}(R_b^+\boldsymbol{\sigma}L_b + L_b^+\boldsymbol{\sigma}R_b),$$

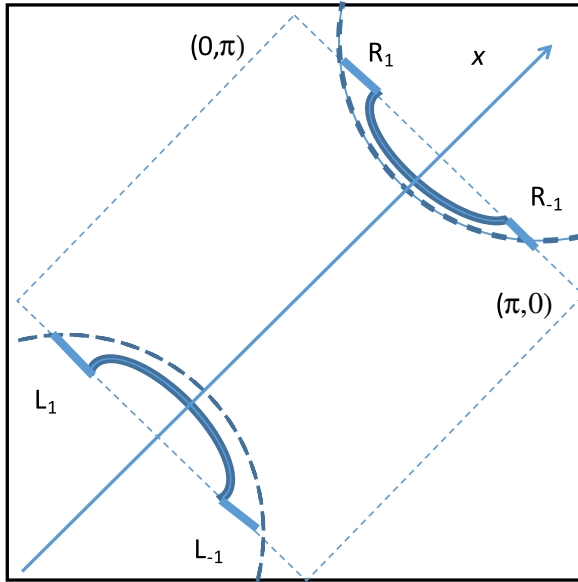$$\gamma = rg^2\chi_0, \quad r \sim \xi^{-1}. \tag{3}$$

FIG. 1. A sketch of a part of the Fermi surface with four hot spots. The dashed curves correspond to the Fermi surface of noninteracting electrons. It is energetically advantageous for the interactions to deform the Fermi surface by making it flat at the hot spots to facilitate nesting of the opposite parts of the FS (drawn by the solid lines). The right (left) moving fermions are located near the flat portions of the Fermi surface and are marked by R_1, R_{-1} (L_1, L_{-1}). Hot spots with the same number are connected by the wave vector (π, π). The ones connected by $(\pi, -\pi)$ are not shown. The line with an arrow corresponds to the coordinate axis of x.

There is a similar Hamiltonian for the quartet of hot spots connected by the wave vector $(\pi, -\pi)$. To the first approximation, these two groups of hot spots can be considered independently.

The form of the interaction (3) has the form used in the models of half-filled ladders. These models have been thoroughly studied using nonperturbative methods. Hence, we can go beyond the standard large-N (N is the number of hot spots) approach. The symmetry of the model is $U(1) \times U(1) \times SU(2) \times Z_2$. The $U(1)$ symmetries refer to the charge conservation inside of every patch, the $SU(2)$ symmetry refers to spin, and the Z_2 symmetry refers to the fact that the patches can be interchanged. The renormalization group (RG) calculations demonstrate [13,14] that this original symmetry increases dynamically when the model scales to strong coupling such that at low energies the maximally allowed symmetry, namely, the $O(8)$ symmetry, emerges. The $O(8)$-symmetric Gross-Neveu (GN) model is exactly solvable [15], which allows one to extract a great deal of information. When the bare coupling γ is not small, the symmetry becomes approximate, but many statements remain valid on a qualitative level [16]. It is particularly important for us that, as was established in Refs. [14,17,18], that the symmetry itself does not uniquely fix the ground state properties of the model. This is related to the fact that there are transformations of the Hamiltonian which do not change the excitation spectrum, but do change the observables. In Ref. [18] it was established that these transformations are automorphisms of the $O(8)$ group. As a consequence, the phase

diagram of the ladder includes different phases, some of which are favorable for superconductivity, and some are not (see the discussion in Ref. [19] and in the Supplemental Material [20]). To find out to what part of the phase diagram the interaction scales requires a certain analysis.

The interaction (3) is divided into two parts: inside of a hot spot (labeled by indices ± 1) and between the spots. For the former ones we have

$$
\begin{aligned}
&V_{11} + V_{-1,-1} \\
&= \gamma \sum_{a=\pm 1} [L_\sigma^+ L_\sigma R_{\sigma'}^+ R_{\sigma'} + 3(R_\sigma^+ R_{\sigma'}^+ L_{\sigma'} L_\sigma + \text{H.c.}) \\
&\quad - (L^+ \boldsymbol{\sigma} L)(R^+ \boldsymbol{\sigma} R)]_a.
\end{aligned}
\tag{4}
$$

This part of the interaction contains the umklapp processes which are responsible for the Mott physics. The interaction between the spots resembles the interchain exchange in the ladder model with no interchain tunneling, studied in Ref. [21]:

$$
V_{1,-1} = -\gamma \int dx \mathbf{S}_1(x) \mathbf{S}_{-1}(x).
\tag{5}
$$

We bosonize the model using the standard notations,

$$
\begin{aligned}
R_{p\sigma} &= \frac{\eta_{p\sigma}}{\sqrt{2\pi a_0}} \exp[-i(\varphi_c + p\varphi_f + \sigma\varphi_s + p\sigma\varphi_{sf})], \\
L_{p\sigma} &= \frac{\eta_{p\sigma}}{\sqrt{2\pi a_0}} \exp[i(\bar{\varphi}_c + p\bar{\varphi}_f + \sigma\bar{\varphi}_s + p\sigma\bar{\varphi}_{sf})],
\end{aligned}
\tag{6}
$$

where a_0 is the lattice constant, $p = \pm 1$, $\sigma = \pm 1$, and

$$
\{\eta_a, \eta_b\} = 2\delta_{ab}
\tag{7}
$$

are Klein factors, and $\varphi_a, \bar{\varphi}_a$ are chiral bosonic fields with commutation relations $[\varphi(x), \varphi(y)] = -(i/4)\text{sgn}(x - y)$, $[\bar{\varphi}(x), \bar{\varphi}(y)] = (i/4)\text{sgn}(x - y)$, $[\varphi(x), \bar{\varphi}(y)] = -i/4$. Then we have

$$
V_{1,-1} = \frac{i\gamma}{\pi a_0}(\cos\sqrt{4\pi}\Phi_c + \cos\sqrt{4\pi}\Phi_f)(\boldsymbol{\xi}_R \boldsymbol{\xi}_L - 3\xi_R^0 \xi_L^0).
\tag{8}
$$

The easiest way to see the difference between the phases is to rewrite the model in terms of Majorana fermions (see the Supplemental Material [20] for details). The ones in the spin sector are defined as

$$
\begin{aligned}
\xi_R^1 &= \xi \frac{\cos(\sqrt{4\pi}\varphi_s)}{\sqrt{2\pi a_0}}, \quad \xi_R^2 = \xi \frac{\sin(\sqrt{4\pi}\varphi_s)}{\sqrt{2\pi a_0}}, \\
\xi_R^3 &= \eta \frac{\cos(\sqrt{4\pi}\varphi_{sf})}{\sqrt{2\pi a_0}}, \quad \xi_R^0 = \eta \frac{\sin(\sqrt{4\pi}\varphi_{sf})}{\sqrt{2\pi a_0}},
\end{aligned}
\tag{9}
$$

where $\{\xi, \eta\} = 0$, $\xi^2 = \eta^2 = 1$ are Klein factors. Together with the Majoranas from the charge sector which are made from the chiral components of Φ_c, Φ_f, they comprise an octet of Majorana fermions transforming according to the vector representation of the $O(8)$ group. The original fermions and their antiparticles transform according to irreducible spinor representations of the group. As is clear from a comparison of (6) and (9), the two groups of the fermions are *nonlocal* with respect to each other. However, the introduction of the Majoranas simplifies the Hamiltonian, reducing it to the

Gross-Neveu model form (we set $v_F = 1$),

$$\mathcal{L} = \sum_{a=c,f} (1 + \gamma/\pi)(\partial_\mu \Phi_a)^2 + V$$

$$+ \frac{1}{2} \sum_{a=0}^{3} \left[\xi_R^a (\partial_\tau - i\partial_x) \xi_R^a + \xi_L^a (\partial_\tau + i\partial_x) \xi_L^a \right],$$

$$V = \gamma \left[-\frac{3}{2(\pi a_0)^2} \cos(\sqrt{4\pi}\,\Phi_c) \cos(\sqrt{4\pi}\,\Phi_f) \right.$$

$$+ \frac{i}{(\pi a_0)} (\cos\sqrt{4\pi}\,\Phi_c + \cos\sqrt{4\pi}\,\Phi_f)(\boldsymbol{\xi}_R \boldsymbol{\xi}_L - 3\xi_R^0 \xi_L^0)$$

$$\left. - (\boldsymbol{\xi}_R \boldsymbol{\xi}_L + \xi_R^0 \xi_L^0)^2 \right]. \tag{10}$$

Here, I decided to leave the charge sector in the bosonic form, which makes it easier to operate with the order parameters. This form is manifestly $U(1) \times U(1) \times SU(2) \times Z_2$ symmetric. Two bosonic fields Φ_c, Φ_f describe the charge sector. The spin sector is described by the four Majorana fermions, three of which transform according to the triplet and one according to the singlet representations of the $SU(2)$ group. The Z_2 symmetry is realized as the invariance of the Lagrangian under a sign change of all Majorana fermions. The renormalization group calculations indicate that the interaction scales to strong coupling where it becomes $O(8)$ symmetric. During the flow the coupling at the last term changes sign. The most important fact is that the signs of the cross terms in the interaction, the ones which include $M_s = i(\boldsymbol{\xi}_R \boldsymbol{\xi}_L)$ and $M_{sf} = i\xi_R^0 \xi_L^0$, do not change under RG. This is because these signs determine the character of the ground state, as explained below (see Refs. [19,20]).

The order parameter. Below, I will argue that the paramagnon exchange postulated by the SF model drives the system exactly into the ground state of the d-Mott phase [14]. This is important since this phase is "pregnant" with d-wave superconductivity and it turns out that the SF model has the right form of the interaction for this. Indeed, the corresponding order parameter (OP),

$$\Delta_d = R_{1\uparrow} L_{2\downarrow} - R_{2\uparrow} L_{1\downarrow} - R_{1\downarrow} L_{2\uparrow} + R_{2\downarrow} L_{1\uparrow} = A e^{i\sqrt{\pi}\Theta_c},$$

$$A = [-\cos(\sqrt{\pi}\,\Phi_f)\sigma_1\sigma_2\sigma_3\mu_0 + i\sin(\sqrt{\pi}\,\Phi_f)\mu_1\mu_2\mu_3\sigma_0], \tag{11}$$

has a finite amplitude. Indeed, this OP can be conveniently factorized into the exponent of the dual charge field Θ_c, whose average is always zero in the Mott phase, and the amplitude A. The amplitude has a vacuum average—that is what I mean by the d-Mott phase being pregnant with the superconductivity. The latter one will emerge when the chemical potential will exceed a half of the cooperon gap so that the field Θ_c becomes gapless. To make sure that the above description is correct, let us consider the amplitude more closely. From (10) we see that the vacuum of the theory corresponds to $\Phi_c = \Phi_f = 0$ or $\Phi_c = \Phi_f = \sqrt{\pi}/2$. The mass of Majorana fermions changes its sign when the fields interpolate from one vacuum to another. In the first vacuum we have $\langle\sigma_a\rangle$ ($a = 1,2,3$), $\langle\mu_0\rangle \neq 0$, and in the second one $\langle\mu_a\rangle$ ($a = 1,2,3$), $\langle\sigma_0\rangle \neq 0$ (see the Supplemental Material [20]). Hence, the vacuum average of the amplitude is never zero.

Now recall that the Gross-Neveu model (10) scales to strong coupling and its spectrum is entirely gapped. The exact solution of the $O(8)$-symmetric model yields the spectrum which contains quasiparticles with quantum numbers of the electron (charge $\pm e$, spin $\pm\frac{1}{2}$, and chain index ± 1) and eight Majorana fermions transforming in the vector representation of the group. Among the latter ones are particle-particle bound states with momentum zero and charge $\pm 2e$ (cooperons). According to Konik and Ludwig [17], the correlation function of the OPs (11) in the d-Mott phase contains a pole, so the cooperons are coherent excitations. There are also particle-hole bound states spin density waves (SDWs) which carry momentum (π,π).

The spectral gaps in the ladder are formed as a consequence of discrete symmetry breaking which occurs at $T = 0$. In the d-Mott phase this symmetry is not a translational one. The quasiparticle excitations are kinks, which interpolate between different degenerate ground states. At finite temperature the density of the kinks is finite and the spectral gaps are gradually filled by the thermal fluctuations. This picture corresponds to a gradual filling of the pseudogap, observed in angle-resolved photoemission spectroscopy (ARPES) experiments such as Ref. [3].

Excitations. The correlation functions of the d-Mott phase were studied by Konik and Ludwig [17]. For instance, the single-particle Green's function is

$$G_q = \frac{i\omega + \epsilon_q(k)}{\omega^2 + \epsilon_q^2(k) + \Delta^2(q)}, \tag{12}$$

where k is perpendicular and q is along the FS. The perturbation (the deviation of the actual FS from the flat one) is just a q-dependent chemical potential, so it must be added to $i\omega$: $i\omega \rightarrow i\omega + \delta\epsilon(q,k)$. This makes the resulting Green's function to more closely resemble the YRZ form, although not quite. The applicability of our ladder approximation is restricted by the region of the FS where the chemical potential lies inside the gap, although this statement requires a correction.

As I pointed out above, alongside the single-particle excitations whose spectra are determined by the poles of (12), the GN model also has collective excitations transforming according to the vector representation of the $O(8)$ group. One of these excitations is the cooperon, a bound state of two electrons (holes) with momentum 0. Its spectrum lies below the two-particle continuum, and therefore the cooperon energy will vanish before the single-particle gap is closed. This means that within the current scenario the superconductivity originates from the areas of momentum space close to the tips of the FS pockets. The mechanism is cooperon condensation, as was suggested in Ref. [7]. Another excitation (also gapped) is a coherent spin-1 magnetic excitation centered at (π,π) which can be identified with the upper part of the "hourglass" spectrum of magnetic excitations (see, for instance, Ref. [22]).

In summary, by adopting a hypothesis that the interactions modify the Fermi surface around the hot spots to generate nesting, I demonstrated that the spin fermion model describes the d-Mott phase physics near the hot spots. This result brings together two successful phenomenological approaches.

It also explains the mechanism of the pseudogap formation: The Fermi surface near the hot spots is truncated without translational invariance breaking.

[1] A. Abanov, A. V. Chubukov, and J. Schmalian, Adv. Phys. **52**, 119 (2003).

[2] Y. Wang and A. Chubukov, Phys. Rev. B **90**, 035149 (2014).

[3] H. B. Yang, J. D. Rameau, Z. H. Pan, G. D. Gu, P. D. Johnson, H. Claus, D. G. Hinks, and T. E. Kidd, Phys. Rev. Lett. **107**, 047003 (2011).

[4] S. Badoux, W. Tabis, F. Laliberte, G. Grissonnanche, B. Vignolle, D. Vignolles, J. Beard, D. A. Bonn, W. N. Hardy, R. Liang, N. Doiron-Leyraud, L. Taillefer, and C. Proust, Nature (London) **531**, 210 (2016).

[5] F. Laliberte, W. Tabis, S. Badoux, B. Vignolle, D. Destraz, N. Momono, T. Kurosawa, K. Yamada, H. Takagi, N. Doiron-Leyraud, C. Proust, and L. Taillefer, arXiv:1606.04491.

[6] E. Dagotto and T. M. Rice, Science **271**, 618 (1996).

[7] R. M. Konik, T. M. Rice, and A. M. Tsvelik, Phys. Rev. Lett. **96**, 086407 (2006).

[8] K.-Y. Yang, T. M. Rice, and F.-C. Zhang, Phys. Rev. B **73**, 174501 (2006).

[9] F. H. L. Essler and A. M. Tsvelik, Phys. Rev. B **71**, 195116 (2005).

[10] W. Xu, G. Kotliar, and A. M. Tsvelik, Phys. Rev. B **95**, 121113 (2017).

[11] T. M. Rice, Phys. Rev. B **2**, 3619 (1970).

[12] Y.-H. Liu, W.-S. Wang, Q.-H. Wang, F.-C. Zhang, and T. M. Rice (unpublished).

[13] L. Balents and M. P. A. Fisher, Phys. Rev. B **53**, 12133 (1996).

[14] H. H. Lin, L. Balents, and M. P. A. Fisher, Phys. Rev. B **58**, 1794 (1998).

[15] A. Zamolodchikov and A. B. Zamolodchikov, Phys. Lett. B **72**, 481 (1978).

[16] A. M. Tsvelik, Phys. Rev. B **83**, 104405 (2011).

[17] R. M. Konik and A. W. W. Ludwig, Phys. Rev. B **64**, 155112 (2001).

[18] H. C. Lee, P. Azaria, and E. Boulat, Phys. Rev. B **69**, 155109 (2004).

[19] D. Controzzi and A. M. Tsvelik, Phys. Rev. B **72**, 035110 (2005).

[20] See Supplemental Material at http://link.aps.org/supplemental/10.1103/PhysRevB.95.201112 for phases of the fermionic ladder.

[21] D. G. Shelton and A. M. Tsvelik, Phys. Rev. B **53**, 14036 (1996).

[22] M. Fujita, H. Hiraka, M. Matsuda, M. M. Matsuura, J. M. Tranquada, S. Wakimoto, G. Xu, and K. Yamada, J. Phys. Soc. Jpn. **81**, 011007 (2012).